

# CFD simulation of clearwater scour at complex foundations

N. S. Tavouktsoglou

*HR Wallingford, Wallingford, United Kingdom*

J. M. Harris

*HR Wallingford, Wallingford, United Kingdom and University College London, London, United Kingdom*

R. J. S. Whitehouse

*HR Wallingford, Wallingford, United Kingdom*

R. R. Simons

*University College London, London, United Kingdom*

**ABSTRACT:** Offshore gravity base foundations (GBFs) are often designed with complex geometries. Such structures interact with local hydrodynamics, creating an adverse pressure gradient resulting in bed shear stress amplification and scour in erodible soils. At present, physical modelling and simple prediction equations have been the only practical engineering tool for evaluating scour around these support structures. However, with the increasing computational power of computers and the development of new Computational Fluid Dynamics (CFD) solvers, scour prediction around foundations using CFD is becoming more practical and accurate. In the present work, three-dimensional (3D) numerical modelling has been applied to reproduce local scour around a complex cylindrical base structure under the forcing of a unidirectional current in clearwater scour conditions. The simulations are carried out using a state-of-the-art multi-phase 3D Euler-Lagrange model based on the open source CFD software OpenFOAM. The fluid phase is resolved by solving modified Navier-Stokes equations, which take into consideration the influence of the solid phase, i.e., the soil particles. The solid phase is solved using the multi-phase particle-in-cell (MP-PIC) approach, a method which takes into account the sediment-sediment interaction, while the particles follow Newton's Law of Motion. The present paper also presents physical modelling results for scour around the same type of structure which were conducted for the same hydrodynamic forcing conditions as in the CFD model. The results of the experimental campaign are used to evaluate the ability of the CFD model to predict the: time evolution of scour; the equilibrium scour depth; and, the 3D characteristics of the scour hole. The results show that the present CFD solver has the capacity to predict with good accuracy the evolution of the scour hole and equilibrium scour depth while capturing key morphological features which are not captured by similar software packages.

## 1 INTRODUCTION

Offshore support structures often are designed with geometries which are more complex than a uniform cylinder. Depending on the design and purpose of the structure the foundation may be comprised of a number of different structural elements which can affect the scour process, and thus the overall functionality of the structure.

Numerical modelling of scour historically has started with single-phase simulations based on the assumptions of potential flow theory (Mao, 1986; Li & Chang, 2000). In recent years and with the increase in the computational power of computers two-phase models have started to become more popular due to their ability to better describe and simulate physical processes that single-phase models are unable to (e.g.

the down-flow in front of the pile, lee wake vortices). Two-phase Computational Fluid Dynamics (CFD) models can be distinguished in the following categories:

- Euler-Euler solvers: In these types of solvers both phases (solid and fluid) are solved as a continuum. They are typically solved using cell-averaged quantities with cell sizes which are typically significantly larger than the size of the sediment, which means that the fluid-particle and particle-particle interactions are also solved explicitly. These interactions are of significant importance in the field of scour and thus the explicit treatment of them can result in inaccurate results.

- Lagrangian-Lagrangian models: These models describe both the fluid and sediment phase as discrete particles with different properties. The shortcoming of these methods is that though they can accurately capture the flow-particle and particle-particle interactions they are computationally expensive and are limited by the number of particles which can be simulated. This makes them unsuitable, currently, to solving real world hydraulic engineering problems.
- Euler-Lagrange models: These solvers can solve the fluid phase using the cell-averaged quantities similar to Euler-Euler models but have the advantage of treating the solid phase on a particle to particle basis. This provides a more computational efficient way of treating scour problems.

The present study investigates the effect a non-uniform cylindrical structure has on an erodible bed under the forcing of a unidirectional current, using the fully three-dimensional Euler-Lagrange model ScourFOAM. ScourFOAM is based on the open source CFD platform OpenFOAM. The results from the simulation are compared with laboratory measurements to evaluate the ability of the model to predict the time development of scour, the equilibrium scour depth and the three dimensional morphological features associated with scour around such structures.

## 2 NUMERICAL MODEL DESCRIPTION

ScourFOAM (Li *et al.*, 2014) is a three-phase model (air-fluid-sediment) which solves the three phases simultaneously. The fluid phase is solved using the Reynolds-averaged Navier Stokes equations while the air-fluid interface is resolved using the Volume of Fluid (VoF) approach as described in Jacobsen (2017). The sediment phase is treated using the particle in cell method and the particles are tracked using barycentric algorithms. The interface between the fluid and the sediment is calculated using the threshold volume fraction method while solving for the inter-particle stresses, fluid drag and body forces. The influence of the solid phase on the fluid is accounted for by using the interphase momentum equation.

### 2.1 Flow model

The fluid and air phase in the present model is solved using the VoF method proposed by Rusche (2003). The momentum equation of which reads as:

$$\frac{\partial \rho U}{\partial t} + \nabla \cdot (\rho U U) - \nabla \cdot (\mu \nabla U) - \nabla U \cdot \nabla \mu = -\nabla p_d - g \cdot x \nabla \rho + \sigma_\kappa \nabla \alpha \quad (1)$$

Here  $U$  and  $\rho$  are the ensemble-averaged flow velocity and fluid density;  $\alpha$  is the volume fraction of water;  $p_d$  is the dynamic pressure component of the total pressure ( $p = p_d + \rho g \cdot x$ );  $\sigma_\kappa$  is the mean curvature of the surface of the fluid;  $g$  is the gravitational acceleration;  $x$  is the position vector; and,  $\mu$  is the dynamic viscosity of the fluid.

The present model accounts for the displacement of water by sediment movement through the Cihonski *et al.* (2013) volume exclusion term:

$$T_{ve} = \frac{\partial \rho U}{\partial t} \ln(\theta_f) + U \cdot \nabla \ln(\theta_f) \quad (2)$$

where  $\theta_f$  is the volume fraction of the cell occupied by the fluid.

Finally, the influence of the solid phase on the fluid phase is incorporated in the model through an inter-phase momentum transfer term which is added to the Poisson equation.

### 2.2 Sediment transport model

The particles in the present model are tracked using a barycentric algorithm using the multi-phase particle-in-cell method in a Lagrangian frame. The particle distribution function of Snider (2001) is used to describe the sediment motion which reads as:

$$\frac{\partial \varphi}{\partial t} + \nabla \cdot (\varphi U_p) + \nabla U_p \cdot (\varphi A) = 0 \quad (3)$$

where  $U_p$  is the particle velocity with the subscript  $p$  denoting the particle;

$\varphi$  the particle probability distribution function; and  $A$  is the particle acceleration which is described by:

$$A = D_p (U - U_p) - \frac{\nabla p_p}{\rho_p} + (1 - \frac{\rho_f}{\rho_p})g - \frac{\nabla \tau}{\theta_s \rho_p} \quad (4)$$

Where  $\theta_s$  is the volume fraction occupied by the solid phase;  $\tau$  the inter-particle stress; and,  $D_p$  is the hydrodynamic drag force.

As can be observed in Equation (4) the present model accounts for the effect of the drag exerted on the particle, the pressure gradient, buoyancy and the inter-particle stress gradient, a fact that distinguishes it from other scour solvers.

For dense solid particle fractions (i.e.  $> 5\%$ ) the continuum particle stress model of Harris and Crighton (1994) is used to determine the inter-particle stresses. This makes the model significantly more computationally efficient compared to solvers with Lagrangian collision models. This is because the particle normal stresses are modelled by a continuum calculation of the particle pressure which requires less computational resources.

Finally, the interface between the solid and water phase is calculated using a threshold volume fraction similarly to the air-water interface.

### 2.3 Experimental set-up

The experimental scour data were obtained from Tavouktsoglou *et al.* (2017). The test was carried out in the coastal flume at University College London (UCL). The test was conducted in a clearwater scour regime under the forcing of a unidirectional current in order maintain a simple hydrodynamic regime. This also avoided the formation of bed features upstream of the test section which would lead to the general lowering of the initial bed and, therefore, complicate the determination of the equilibrium scour depth. The dimensions of the flume were 20 m long, 1.0 m deep and 1.2 m wide. A false bed was installed 0.25 m above the existing flume base with a 2 m recess at the middle which served as a sand pit where scour could develop freely. The test structure was placed in the centre of the flume at a distance approximately 10 m from the flume entrance. The flow velocity and water depth were controlled through a set of recirculating pumps. The present test examined the scour development around a cylindrical base structure with a base diameter of 0.2 m, a stick-up height of 0.09 m and top shaft diameter of 0.07 m (see Figure 1). Table 1 provides a summary of the main flow conditions used in this study, which will also be used in the numerical simulation.

Table 1: Summary of flow conditions used in experimental and numerical study

$U$ (m/s)	$h$ (m)	$D_{base}$ (m)	$d_{50}$ (mm)
0.245	0.35	0.2	0.2

### 2.4 Numerical set-up

The mesh used in this study was selected to have the same dimensions as the flume in which the experimental measurements were made. Thus the numerical flume was 20 m long 1.2 m wide and 0.5 m deep. The mesh was comprised of a total of 1,500,000 cells with

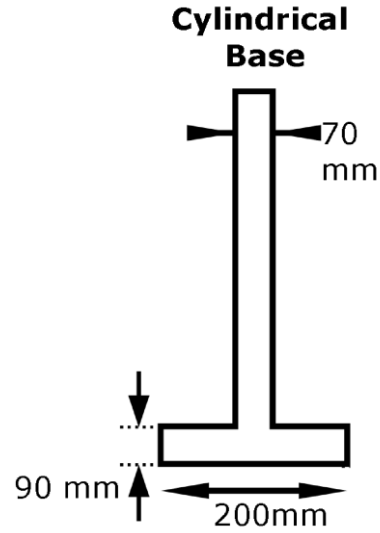


Figure 1: Dimensions for cylindrical base structure geometry used in this study

an increasing refinement closer to the structure (see Figure 2a). This was done to capture as accurately as possible the flow separation off the structure's surface. The sediment box (i.e. Lagrangian field) is populated by 2,000,000 particles confined in a 0.5 x 0.5m inverted pyramid surrounding the base of the structure in the centre of the domain (see Figures 2a and b). The inverted pyramid was selected to reduce the amount of Lagrangian particles needed to fill the virtual sand pit and thus reduce the computational time.

To capture turbulent effects, the  $k-\omega$  turbulence model was used. The dimensions of the structure were taken from Tavouktsoglou *et al.* (2017) and are shown in Figure 1.

## 3 RESULTS

### 3.1 Current profile

Given that the scour characteristics around complex structures are dependent on the incoming flow profile (Tavouktsoglou *et al.*, 2017), a comparison between the measured and computed flow profiles are given in Figure 3. It can be observed that the flow profiles have the same mean value but do deviate. With the measured flow having smaller velocities near the bed and higher values closer to water surface when compared to the simulated flow. This is attributed to the fact that in the experimental set-up only a small portion of the flume's bed near the test section was covered by a roughened false bed. While in the numerical flume the entire domain's bed had a roughness equal to that of the tested sand. An additional factor contributing to this discrepancy is the flow inlet of the flume which is upwards facing, this translates to slightly

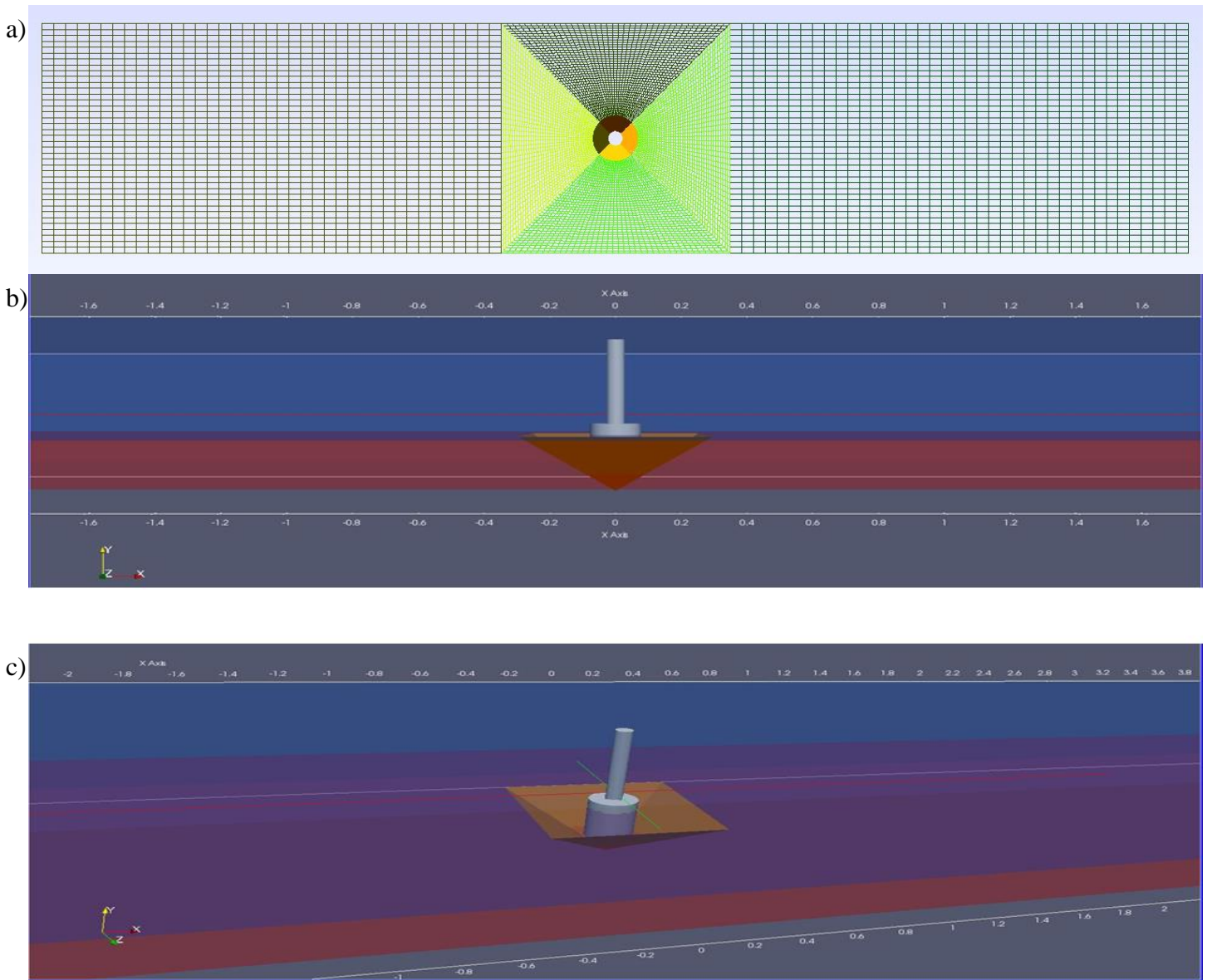


Figure 2: Numerical flume set-up: a) Numerical mesh; b) & c) close-up of the numerical scour pit (transparent blue water phase, transparent red immobile bed and orange sediment pit)

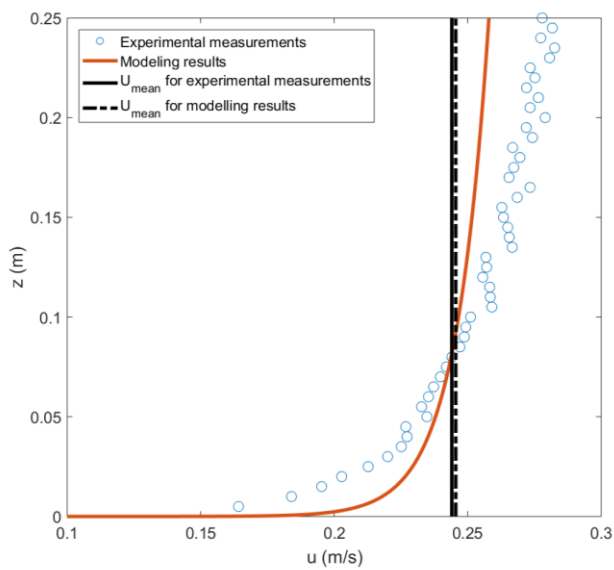


Figure 3: Flow profiles for numerical and experimental results, with corresponding depth averaged values

larger flow velocities near the water surface compared to an inlet which is facing in the principal flow direction. This means that it is expected that the numerical results would yield a more well developed flow profile, in this case with a thinner boundary layer.

### 3.2 Equilibrium scour depth

The equilibrium scour depth induced by a structure is the most important engineering aspect of scour. Numerous empirical methods for the prediction of the equilibrium scour depth exist which can be applied with some success but their shortcoming is that they cannot provide an estimate of the overall 3D scour features. This section presents the results of the numerical simulation and provides a comparison with experimental measurements for a cylindrical base structure. Figure 4 presents the results of this comparative study.

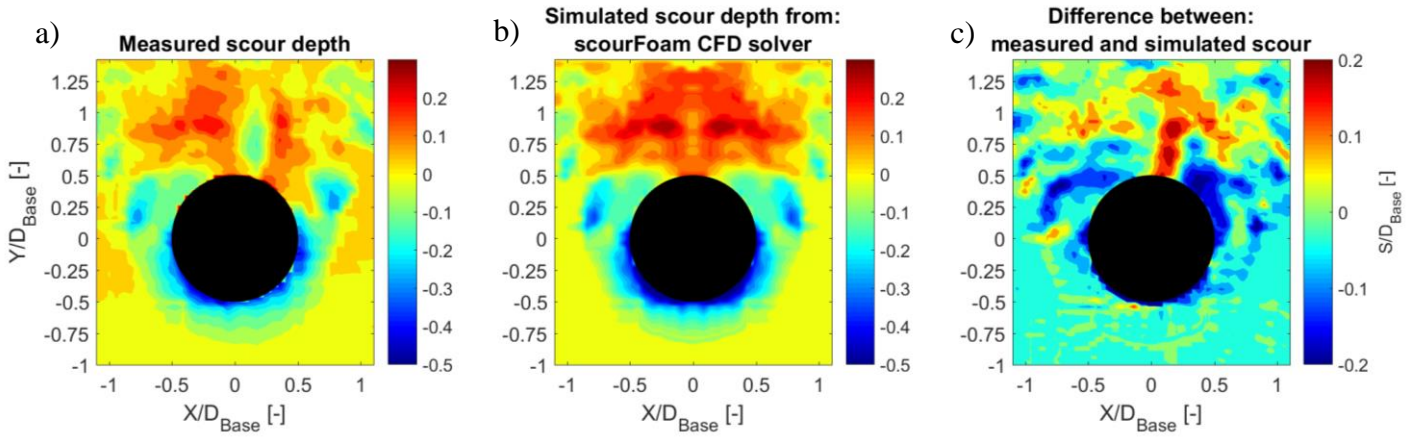


Figure 4: Three dimensional scour around cylindrical base structure: A) Experimental measurements; b) Numerical simulation; and c) Difference between measured and simulated

As can be seen the numerical model predicts well the 3D scour around the structure. The discrepancies and variation shown in Figure 4c are mainly attributed to the slight variation of the location of scour features in the x-y plane rather than the underestimation or overestimation of scour. This is expected as the locations of these features are highly effected by the slightest of variations in the starting flow and bed conditions. It can be seen that the maximum scour depth in both cases occurs at an angle of 45 degrees relative to the flow direction which agrees with potential flow theory. There is a small tendency for the model to over predict the equilibrium scour depth in front of the structure. This is mainly attributed to the slightly different flow profile which is used in the numerical model. According to Tavouktsoglou *et al.* (2017) higher near-bed velocities (as is the case in the numerical model) induce a stronger depth-averaged horizontal pressure gradient and thus deeper scour

depths. Further observation of the data reveals that the model captures accurately the lateral extent of the scour hole both in the streamwise and cross-flow direction. This aspect is also important for design purposes as it controls the lateral extent of the scour protection. Therefore, the overestimation of the extent of the scour hole may lead to the overdesign of the scour protection system. In the case of the underestimation of the scour extent, the scour protection may be designed to be less extensive than required and thus pose a threat to the stability of the foundation.

The present solver also captures accurately the secondary scour holes which radiate away from the structure at an angle  $\pm 130$  degrees relative to the flow direction at the lee of the structure. This scour feature is associated with the lee-wake vortices which are induced by the flow structure interaction and are a common feature in cylindrical geometries (Olsen & Melaen, 1993). These secondary scour features are

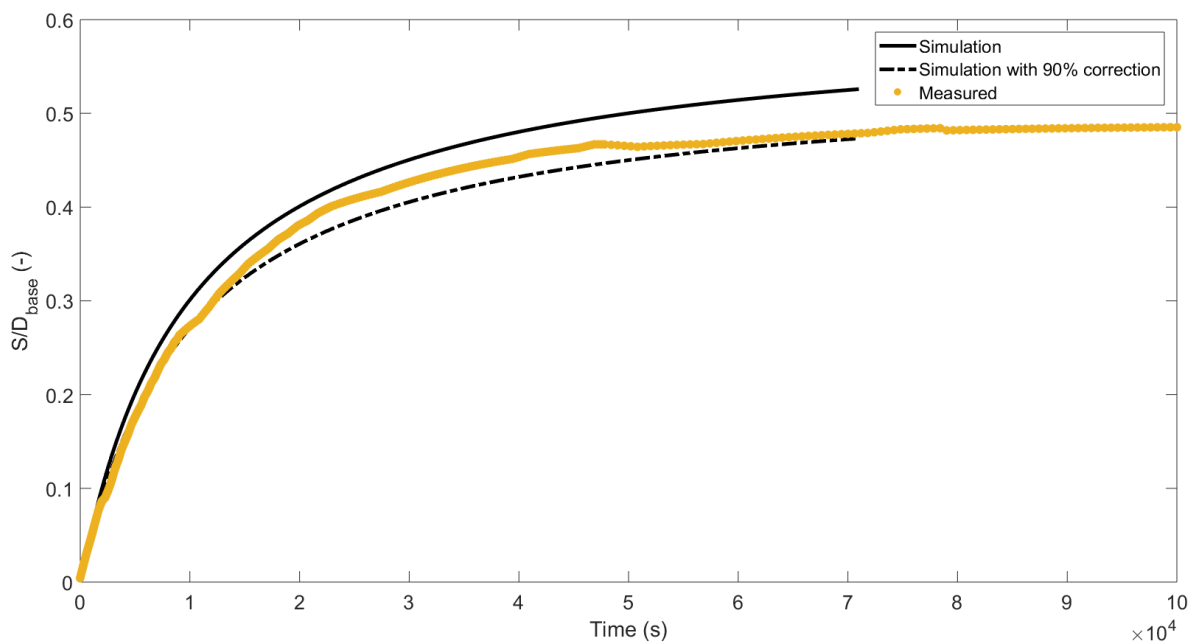


Figure 5: Time development of scour for experimental; numerical results; and corrected numerical results

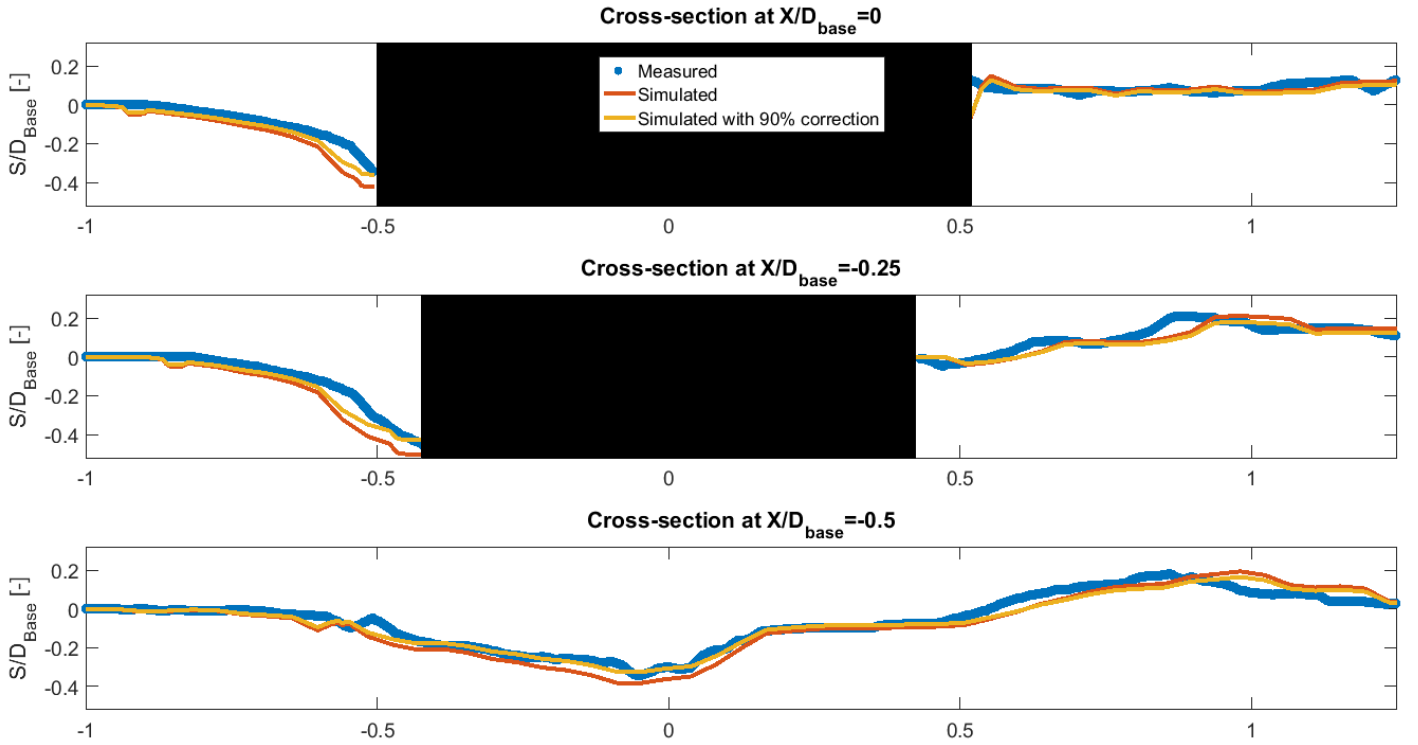


Figure 6: Cross-sectional plots of the scour depth for the experimental, numerical and corrected numerical results at  $X/D_{base} = 0$ ,  $X/D_{base} = -0.25$  and,  $X/D_{base} = -0.5$

also of significance for the design of scour protection systems as they may destabilize the edge detail of the scour protection and thus make the entire protection susceptible to failure. The simulation of this feature is also important as many existing sediment transport solvers have difficulties reproducing.

A final feature which is picked-up by the present model and shows its ability to accurately capture the physical processes associated with scour around complex geometries is the deposition zone at the lee of the structure. This feature is caused by a secondary scour mechanism, the counter-rotating streamwise phase-averaged vortices (LSCSVs), which effectively creates a strong upward pressure gradient which re-suspends sediment from the lee of the structure. The LSCSVs are mainly driven by the longitudinal counter-rotating vortices which are created partly by the horseshoe vortex and the variation of the shedding frequency over the height of the structure (Baykal *et al.*, 2015). In the case of the cylindrical base structure the interaction between the flow and the components of the foundation with different diameters leads to the disruption of the LSCSVs. This in turn, reduces the erosion rate at the lee of the structure and thus more deposition takes place. Figure 4a shows that the sediment mound at the lee of the structure is not in line with the principal flow axis. This is attributed to a small flow asymmetry of order 5% which was present in the flume. A closer examination of this feature shows that the depression in the middle of this deposition zone is deeper in the case of the experimental results. This is also explained by the flow asymmetry

which produces a stronger lee wake vortex on one side and thus a stronger upward flow gradient at the lee.

### 3.3 Time development of scour

After the pile is installed the scour depth develops rapidly; however, it is important to predict the time evolution of scour for several reasons:

- To determine the scour development during a storm or extreme flood event;
- To calculate the time window available to install scour protection after the foundation is installed; and
- To evaluate the total scour depth in layered and mixed sediments.

Numerous methods for predicting the time evolution of scour around monopiles have been developed (Harris *et al.*, 2010 contains a brief review). The shortcoming of these methods is that they have all been developed based on laboratory data. This means that their accuracy is subject to scale effects and their performance varies from case to case. Therefore, the accurate prediction of the scour development using a numerical model can provide a useful tool in the hands of a designer. Figure 5 presents the results of the comparison between the experimental and numerical results. In this figure the scour depth is measured adjacent to the structure at an angle of 45 degrees relative to flow direction. It can be seen that the present

model predicts well the time development of scour. The model has a tendency to over predict the scour but this is attributed to the stronger pressure gradient induced by the flow in the case of simulation.

### 3.4 Application of correction factor to numerical results

In sections 3.2 and 3.3 it was that the present model has the tendency to over-predict the scour depth around the structure. The difference between experimental and numerical results is small enough to be attributed to the slightly different flow profiles that were present in each case. To verify this, the scour prediction correction factor of Tavouktsoglou *et al.* (2016) is applied to the simulation data. Table 2 provides a summary of the data used in this analysis:

Table 2: Summary of data used for the calculation of the correction factor

Name	$\langle Eu \rangle$	$K$
Simulated	0.35	0.636
Measured	0.27	0.574

In the data above  $\langle Eu \rangle$  is the depth-averaged pressure gradient and can be calculated using the method outlined in Tavouktsoglou *et al.* (2016), and  $K$  is the resulting correction factor. From Table 2 it can be seen that the difference of  $K$  between the simulated and measured cases is 90%. Therefore, by applying a 90% correction factor to the simulation results we can obtain a corrected time development curve. The dashed line in Figure 5 shows that the agreement between the two data-sets has significantly improved, with the numerical solution following more closely but slightly underestimating the scour depth during the stabilization phase of the measured process.

The same correction factor of 90% is applied to three representative cross-sections of the 3D scour measurements (see Figure 6). The cross-sections correspond to lines with  $X/D_{base} = 0$ ,  $X/D_{base} = -0.25$  and,  $X/D_{base} = -0.5$ .

As can be seen the original simulation has the tendency to over-predict the scour depth in front of the structure. With the application of the correction factor the agreement between the two data-sets improves considerably. There is a small discrepancy with regards to the upstream slope but this may be attributed to the natural variation of the sediment particles used in the experiments.

At the lee of the pile it can be seen that the model captures well the deposition zone in the three cross-section presented here, though the numerical solution

tends to produce bedforms which have a larger length than the ones observed in the experiments. As mentioned in section 3.2 these morphological features are very sensitive not only to the initial flow and bed conditions but also on the lee-wake field which in turn is effected by the selected turbulence model.

## 4 CONCLUSIONS

In this study the local scour around a cylindrical based structure was investigated numerically using Scour-FOAM, a state-of-the-art Euler-Lagrange multi-phase CFD solver. The advantage of this model is its ability to closely simulate the physical properties of the sediment while being numerically efficient. The numerical model was set-up to replicate a physical modelling flume. The calculated scour was then compared to laboratory measurements and a good agreement was found. The following conclusions can be made from this study:

- The numerical model captures well the three dimensional scour features associated with complex structures.
- The equilibrium scour depth is predicted with good accuracy considering the small variations between the numerical and experimental set-up.
- The time development of scour is captured very well by the present model
- Small discrepancies in the incoming flow profile can lead to significant differences in the resulting scour depth.

## 5 ACKNOWLEDGEMENTS

The authors would like to thank HR Wallingford and Dr. Aggelos Dimakopoulos for their valuable input and funding for this research project.

## 6 REFERENCES

- Andrews, M. J., & O'rourke, P. J. (1996). The multiphase particle-in-cell (MP-PIC) method for dense particulate flows. *International Journal of Multiphase Flow*, 22(2), 379-402.
- Baykal, C., Sumer, B. M., Fuhrman, D. R., Jacobsen, N. G., & Fredsøe, J. (2015). Numerical investigation of flow and scour around a vertical circular cylinder. *Phil. Trans. R. Soc. A*, 373(2033), 20140104.

Cihonski, A. J., Finn, J. R., & Apte, S. V. (2013). Volume displacement effects during bubble entrainment in a travelling vortex ring. *Journal of Fluid Mechanics*, 721, 225-267.

Harris, J.M. Whitehouse, R.J.S. and Benson, T. (2010). The time evolution of scour around offshore structures. *Proceedings of the Institution of Civil Engineers, Maritime Engineering*, 163, March, Issue MA1, 3 – 17.

Harris, S. E., & Crighton, D. G. (1994). Solitons, solitary waves, and voidage disturbances in gas-fluidized beds. *Journal of Fluid Mechanics*, 266, 243-276.

Jacobsen, N. G. (2017). *waves2Foam Manual*.

Li, F., & Cheng, L. (2000). Numerical simulation of pipeline local scour with lee-wake effects. *International Journal of Offshore and Polar Engineering*, 10(03).

Mao, Y. (1987). The interaction between a pipeline and an erodible bed. *Series Paper Technical University of Denmark*, (39).

Olsen, N. R., & Melaaen, M. C. (1993). Three-dimensional calculation of scour around cylinders. *Journal of Hydraulic Engineering*, 119(9), 1048-1054.

Rusche, H. (2003). *Computational fluid dynamics of dispersed two-phase flows at high phase fractions (Doctoral dissertation, Imperial College London (University of London))*.

Snider, D. M. (2001). An incompressible three-dimensional multiphase particle-in-cell model for dense particle flows. *Journal of Computational Physics*, 170(2), 523-549.

Tavouktsoglou, N. S., Harris, J. M., Simons, R. R., & Whitehouse, R. J. (2016, June). Equilibrium scour prediction for uniform and non-uniform cylindrical structures under clear water conditions. In *ASME 2016 35th International Conference on Ocean, Offshore and Arctic Engineering* (pp. V001T10A007-V001T10A007). American Society of Mechanical Engineers.

Tavouktsoglou, N. S., Harris, J. M., Simons, R. R., & Whitehouse, R. J. S. (2017). Equilibrium Scour-Depth Prediction around Cylindrical Structures. *Journal of Waterway, Port, Coastal, and Ocean Engineering*, 143(5), 04017017.

Li, Y., Kelly, D. M., Li, M., & Harris, J. M. (2014). Development of a new 3D Euler-Lagrange model for the prediction of scour around offshore structures. *Coastal Engineering Proceedings*, 1(34), 31.